A CO SURVEY OF THE DARK NEBULAE IN PERSEUS, TAURUS, AND AURIGA

H. UNGERECHTS AND P. THADDEUS
Goddard Institute for Space Studies and Columbia University
Received 1986 February 20; accepted 1986 September 4

ABSTRACT

A region of 750 square degrees including the well-known dark nebulae in Perseus, Taurus, and Auriga was surveyed in the 115 GHz, $J = 1-0$ line of CO at an angular resolution of $0°5$. The spectral resolution of the survey is 250 kHz, or 0.65 km s^{-1}, and the rms noise per spectrometer channel is 0.14 K. Emission was detected from nearly 50% of the observed positions; most positions with emission are in the Taurus-Auriga dark nebulae, a cloud associated with IC 348 and NGC 1333, and a cloud associated with the California nebula (NGC 1499) and NGC 1579, which overlaps the northern Taurus-Auriga nebulae but is separated from them in velocity. Other objects seen in this survey are several small clouds at Galactic latitude $-25°$ to $-35°$ southwest of the Taurus clouds, and the L1558 and L1551 clouds in the south. The mass of each of the IC 348 and NGC 1499 clouds is about 5×10^4 $M_\odot$, and that of the Taurus-Auriga clouds about 3.5×10^4 $M_\odot$; the total mass of all clouds surveyed is about 2×10^5 $M_\odot$. On a large scale, the rather quiescent Taurus clouds are close to virial equilibrium, but the IC 348 and NGC 1499 clouds are more dynamically active. Several small clouds with virial masses 10–30 times their CO masses are similar to the diffuse molecular clouds at high Galactic latitudes.

Subject headings: interstellar: molecules — nebulae: general — nebulae: H II regions

I. INTRODUCTION

The extensive complex of dark nebulae in Perseus, Taurus, and Auriga is one of the best examples of nearby molecular clouds in which the formation of stars, particularly those of low mass, can be observed. These clouds are close enough to be studied in great detail, not only with moderate-aperture optical and infrared telescopes but also with single-antenna radio telescopes. In this paper we present a complete survey in the CO 1–0 line of the conspicuous obscurations in Taurus and Auriga; the star-forming cloud complex in Perseus related to IC 348, NGC 1333, and the Per OB2 association; and a cloud extending from the California nebula (NGC 1499) in Perseus along NGC 1579 and LkHα 101 well into Auriga. While young stars with rather high luminosity are associated with the IC 348 cloud, only low-mass stars, e.g., T Tauri stars, are found near the Taurus and Auriga clouds (see, e.g., Jones and Herbig 1979; Cohen and Kuhi 1979).

Radio observations of molecules in the Taurus clouds began with Heiles's (1968) detection of normal OH emission in a region of high extinction near R.A. 4^h38^m, decl. $25°18'$, afterward known as Heiles Cloud 2. In the same region, the 6 cm H$_2$CO absorption line was discovered by Palmer *et al.* (1969); Kutner (1973) observed this line at selected positions in the dark filament southwest of Heiles Cloud 2, now sometimes called Kutner's cloud. More extensive H$_2$CO observations there were later made by Heiles and Katz (1976) and Sume, Downes, and Wilson (1975), but the lines they observed were too weak to establish a connection between Heiles Cloud 2 and Kutner's cloud. In a few locations in Taurus (e.g., in the well-known source TMC-1, a core of Heiles Cloud 2), radio spectroscopy has provided evidence of a surprisingly complex chemistry (e.g., Broten *et al.* 1978;

Toelle *et al.* 1981; Thaddeus *et al.* 1985; Thaddeus, Vrtilek, and Gottlieb 1985), and infrared observations (Benson, Myers, and Wright 1984; Beichman *et al.* 1986) have shown that low-mass stars have formed in or near a significant fraction of these dense cores. All cores lie in regions of high visual extinction which tend to appear on optical photographs as long, extended, dark filaments (Barnard 1927).

A complete survey of the molecular clouds in this region is highly desirable as a prerequisite to realistic estimates of the total masses, interpretations of the *IRAS* survey, and a general understanding of the structure and dynamics of the clouds. During the past decade, CO maps have become accepted as the best currently available tool to survey the distribution of molecular gas. Although CO emission was detected in Heiles Cloud 2 soon after the first detection of the $J = 1-0$ line in interstellar space (Wilson, Jefferts, and Penzias 1970; Penzias *et al.* 1972), to date no complete, unbiased survey of this region has been done. Most CO maps in Taurus have been limited to selected areas, such as the dark filaments (e.g., Baudry *et al.* 1981; Myers 1982; Kleiner and Dickman 1984; Murphy and Myers 1985; Duvert, Cernicharo, and Baudry 1986). The available CO maps of the other clouds cover only some active regions with high line intensities; see, e.g., Sargent (1979) for the IC 348 cloud and Elmegreen and Elmegreen (1978) for the region near NGC 1499. The most extensive previous CO study (Baran 1985) is severely undersampled and suffers from a rather poor spectral resolution of 2.6 km s^{-1}. So far, the OH survey by Wouterloot and Habing (1985) gives the best picture of the large-scale distribution of the clouds with $b > -20°$, but their map was limited to the regions where Baran had detected CO.

A new SIS receiver with an extremely low noise temperature now used on the Columbia 1.2 m telescope allows us to

map CO rapidly with full sampling. This paper presents the results of a survey for which the angular resolution of the telescope was reduced to $0°.5$, allowing the observations for the complete region to be finished within four months, while sufficient resolution was retained to see significant substructure, e.g., the dark filaments in Taurus. Further, this angular resolution is adequate for comparisons on a large scale of the CO distribution with γ-ray (*COS B*), A_V, H I, and infrared (*IRAS*) surveys.

We describe the instrument and the observational methods in § II, then comment on the major features in our maps and on selected individual clouds in § III. The available distance estimates for the clouds and our best current estimates of structure and mass are discussed in § IV. Appendix A explains the analysis of frequency-switched CO spectra, and more detailed descriptions of some individual clouds are given in Appendix B.

II. OBSERVATIONS AND ANALYSIS

The observations were made in 1985 February–May in New York City with the Columbia millimeter-wave telescope, which has a full beamwidth at half-maximum of $8°.7$ at 115 GHz, the frequency of the CO $J = 1-0$ transition. The spectrometer, a 256 channel, 250 kHz filter bank, provided a velocity resolution of 0.65 km s^{-1}. The front end was a single-sideband SIS receiver (Pan 1984), with a receiver noise temperature of typically ≤ 90 K and a total system noise temperature ≤ 600 K.

In order to cover a large area quickly, the angular resolution of the telescope was reduced to a $0°.5 \times 0°.5$ beam by stepping the telescope during each scan through a 4×4 square raster of positions separated by $\frac{1}{8}°$ —slightly less than the beamwidth. Telescope pointing was established to better than $1'$ by observing stars with a small, coaligned optical telescope, and was checked regularly by radio continuum observation of the Sun. The intensity of the spectra was calibrated and corrected for atmospheric absorption by rotating a room-temperature blackbody chopper wheel in front of the feed before each scan (Cohen 1978; Kutner 1978). The temperature and opacity of atmospheric water vapor were measured by antenna tipping daily when the weather was stable and more often when it was variable. A correction for beam efficiency was applied to obtain intensities that are in agreement with the Columbia survey of Orion and Monoceros (Maddalena *et al.* 1986), which Bloemen *et al.* (1984) used to derive the conversion from integrated CO intensity to H$_2$ column density for nearby molecular clouds, and are within 5% of all other Columbia data reported since 1980. Although recently Bronfman *et al.* (1986) estimated that the intensities reported here are about 20% below the true radiation temperature (i.e., the temperature of a blackbody that just fills the main beam), for consistency we retain the scale used for the CO mass calibration. Pointing and calibration were checked daily using localized CO sources (e.g., peaks 8a, 12a, and 27f in Table 1). Since the lines in all clouds surveyed are rather narrow, we were able to save time by frequency switching (see Appendix A for details). Integration times were automatically set to achieve an rms noise (after folding and summing over both

frequency-switched components) of ≤ 0.14 K, which under good weather conditions typically required 1 minute.

A total of 3817 CO spectra were taken, covering ~ 750 square degrees. All positions are on a regular coordinate grid every 2^m in right ascension and $0°.5$ in declination. No cosine correction was applied, so the step in right ascension is somewhat less than $0°.5$ in true angle, decreasing slightly with declination. Sampling is on the full $2^m \times 0°.5$ grid for most of the survey, but small areas in the northwestern and southwestern corners are undersampled, $4^m \times 1°$, since no emission was detected. The total area covered is outlined in Figure 1. No data were taken at declinations below $16°$, a region extensively mapped by Maddalena *et al.* (1986) in the Orion-Monoceros survey, or within $4°$ of the Galactic plane to the northeast covered in the Columbia survey of the second Galactic quadrant (Gottlieb, Brock, and Thaddeus 1986).

Most of the spectra in our survey are readily summarized because the structure of the lines is generally simple. We consider a spectral feature to be a line if its peak intensity is greater than 0.3 K and its integrated intensity is greater than 0.5 K km s^{-1}; if it is not a single strong channel, or spike; and if it is not at the velocity expected for the telluric line. Four parameters were calculated for all positions where the observed spectrum has at least one detected line: the peak line temperature T_R, the integrated line intensity $W_{CO} = \int T_R \, dv$, the equivalent width $\Delta v_{equ} = W_{CO}/T_R$, and the average velocity $v_{av} = \int T_R(v) v \, dv / W_{CO}$. The integrals are over the range where $T_R > T_{rms} = 0.14$ K. At positions with multiple lines these parameters were calculated for each line separately as well as for the total emission. We define two spectral peaks as two distinct lines if they are separated by at least three channels and a minimum lower than 60% of the lower and 30% of the higher peak intensity. Although these values are somewhat arbitrary, they provide a criterion which agrees well with a subjective and qualitative discrimination of double lines, as opposed to blends, and was therefore used consistently at all positions in this survey. With the possible exception of the confused region near NGC 1499, the criterion adopted is sufficiently stringent that all double lines are probably from separate emitting clouds rather than from self-absorption by foreground matter.

III. RESULTS

Maps of velocity-integrated intensity and average line velocity give a fairly complete summary of the results from our survey, because the velocity structure of the lines is generally simple, with single lines at about 90% of the positions where CO was detected. We show W_{CO} as a contour plot in Figure 1 and as a false-color map in the upper part of Figure 2 (Plate 44); for comparison, the line peak temperature, T_R, is also shown in false color in the lower part of Figure 2. The best format to display the velocity structure is a false-color map, following the standard astronomical convention of red for redshift and blue for blue (Fig. 3, *top* [Pl. 45]). To show the relation to optical objects, in Figure 4 the locations of selected well-known nebulae from the *New General Catalogue* and the *Index Catalogue* (Dreyer 1888, 1895, 1908; Sulentic and Tifft 1973), Sharpless's (1959) catalog of
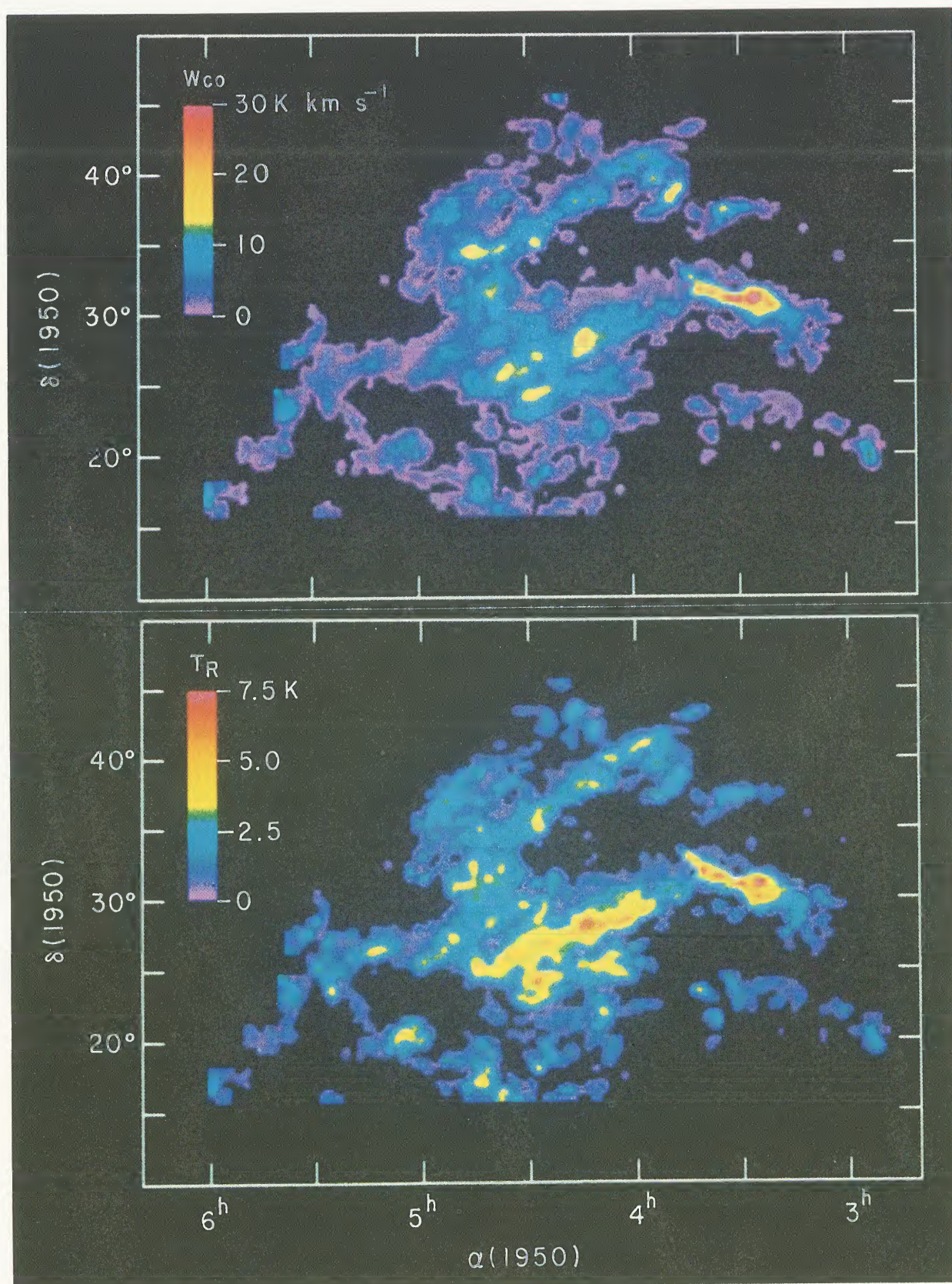
PLATE 44

FIG. 2.—False-color maps of integrated CO intensity, W_{CO} (*top*), and CO peak line temperature, T_R (*bottom*). A two-dimensional spline interpolation to a 0°1 × 0°1 raster was applied to the measured data to produce a smooth color distribution.
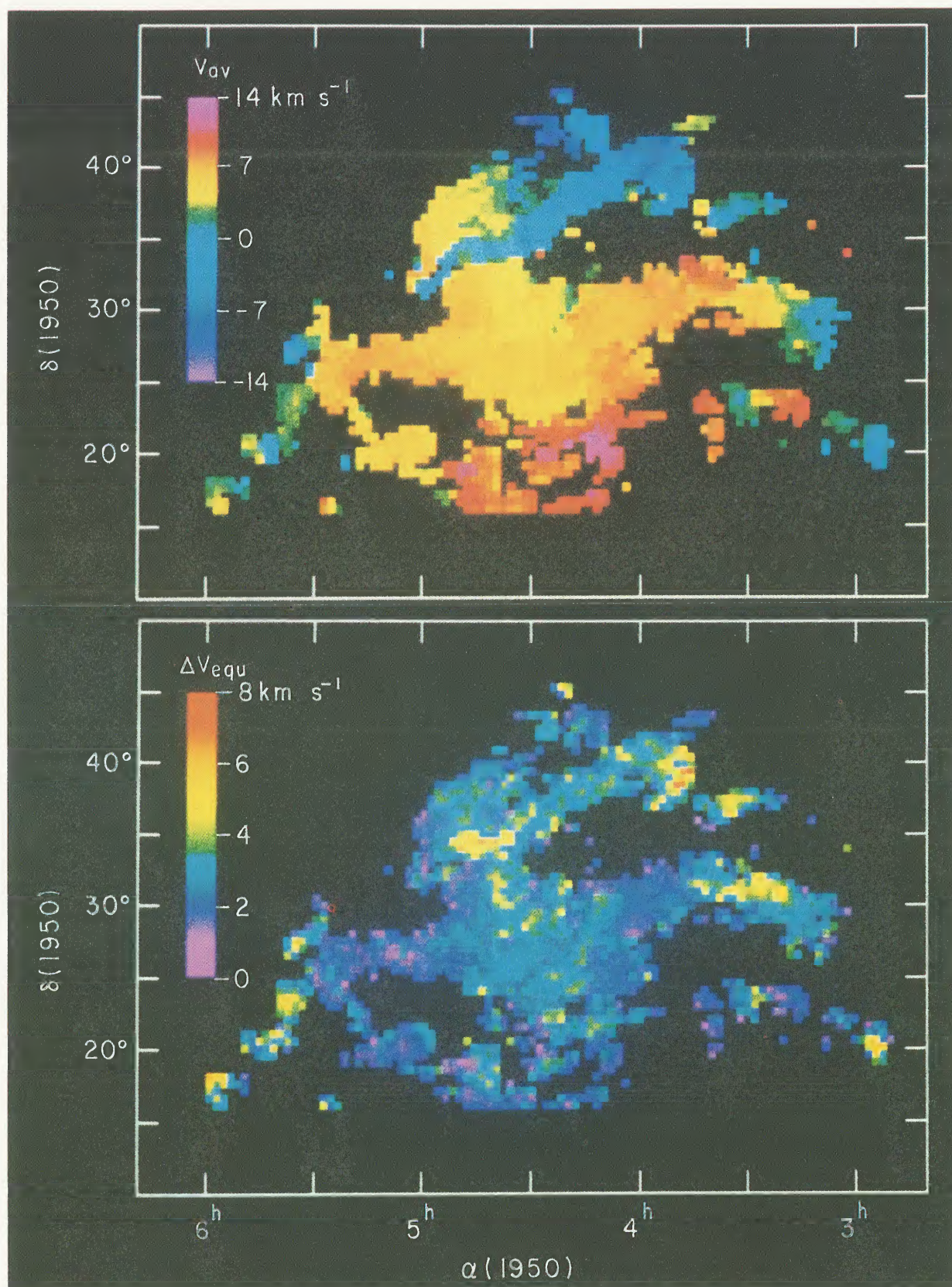
UNGERECHTS AND THADDEUS (*see* page 646)

PLATE 45

FIG. 3.—False-color maps of the average CO line velocity, v_{av} (averaged over all velocity components; *top*), and the line equivalent width, Δv_{equ} (*bottom*). Here no interpolation was applied, and the sampling pixels ($2^m \times 0°5$) are clearly seen.

UNGERECHTS AND THADDEUS (*see* page 646)

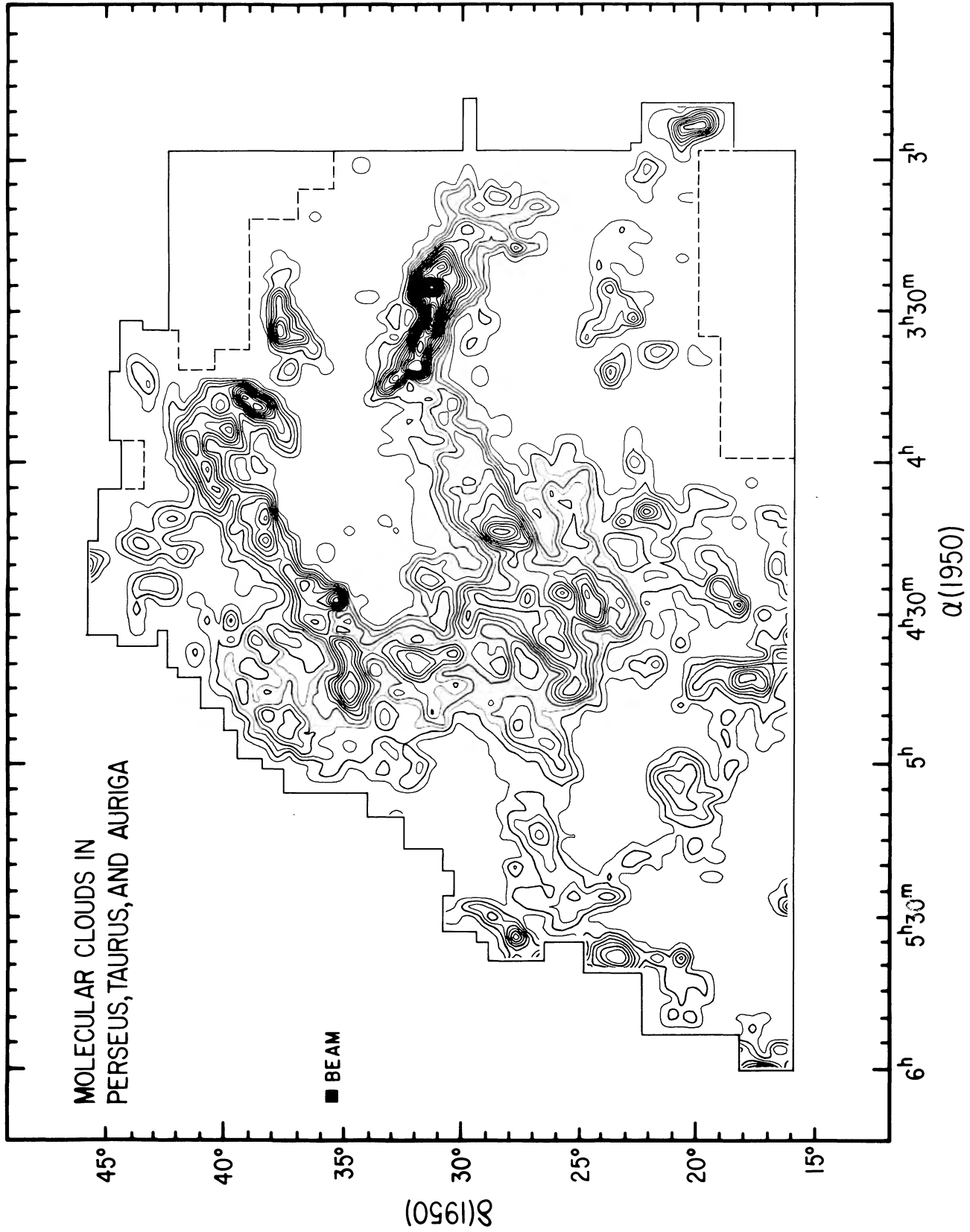MOLECULAR CLOUDS IN
PERSEUS, TAURUS, AND AURIGA

■ BEAM

FIG. 1.—Velocity-integrated intensity of CO emission, W_{CO}. The lowest contour is 0.5 K km s^{-1}, and the separation between contours is 1.5 K km s^{-1}. The border of the surveyed region is indicated by the outer, solid line; in the small regions beyond the dashed line the map is undersampled, with a spacing of $4^m \times 1°$.
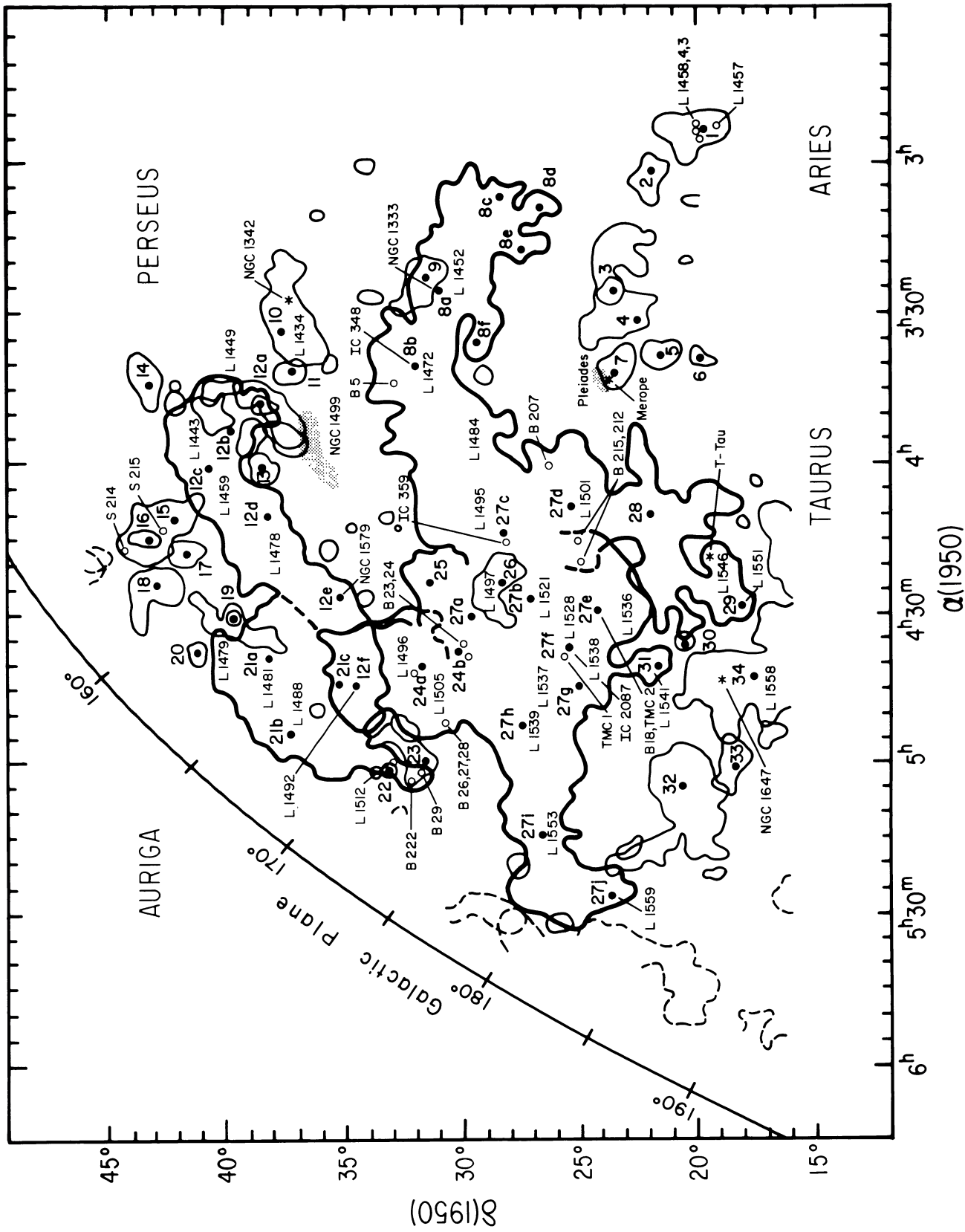
PERSEUS

ARIES

AURIGA

TAURUS

Pleiades

Merope

T-Tau

Galactic plane

$\alpha(1950)$

$\delta(1950)$

3^h 3^h30^m 4^h 4^h30^m 5^h 5^h30^m 6^h

$45°$ $40°$ $35°$ $30°$ $25°$ $20°$ $15°$

$160°$ $170°$ $180°$ $190°$

NGC 1342 NGC 1333 NGC 1499 NGC 1579 NGC 1647
IC 348 IC 359 IC 2087
B 5 B 207 B 215,212 B 23,24 B 26,27,28 B 29 B 222 B 18,TMC 2

L 1458,4,3 L 1457 L 1452 L 1472 L 1449 L 1443 L 1459 L 1478 L 1484 L 1495 L 1501 L 1521 L 1528 L 1536 L 1538 L 1537 L 1541 L 1546 L 1551 L 1558 L 1559 L 1553 L 1505 L 1496 L 1479 L 1481 L 1488 L 1492 L 1512 L 1497 L 1539 L 1647 L 1434
S 214 S 215
TMC I

FIG. 4.—Designation of clouds and CO peaks (*full circles*; *large labels*) and locations of various objects from the NGC, IC, Lynds, and Barnard catalogs (*small labels*). Cloud outlines correspond to the 0.5 K km s^{-1} level of W_{CO}.

H II regions, and Barnard's (1927) and Lynds's (1962) catalogs of dark nebulae are shown against the lowest W_{CO} contour from Figure 1.

Three major molecular clouds dominate the maps: (1) the long northern cloud at negative velocities in Perseus and Auriga, which is associated with the California nebula (NGC 1499) and NGC 1579 and has a distance of 350 pc; (2) the Taurus dark clouds in the center of our survey with a major extension north into Auriga, which have velocities of 5–8 km s^{-1} and a distance of 140 pc; and (3) the IC 348 cloud, which lies west of the Taurus clouds, mainly in Perseus and Aries, at a distance of 350 pc with velocities varying rather systematically from 10 to 0 km s^{-1} (for a discussion of distance estimates see § IVa). The IC 348 cloud is also known as the Per OB2 cloud (Sancisi *et al.* 1974; Sargent 1979), because it is believed to be related to the Per OB2 association located mainly in the area free of CO to the northeast with only a few stars in the direction of the cloud. Both W_{CO} and T_R are strongest at the position of NGC 1333, a bright nebula in a region of active star formation. A fairly large isolated cloud (L1434) at velocity 0–3 km s^{-1} lies about 6° north of IC 348 toward the open star cluster NGC 1342.

Northeast of the IC 348 cloud beyond the large CO hole around Per OB2 there is strong CO emission with broad multiple lines, mostly at negative velocities, near 3$^{\rm h}$50$^{\rm m}$, 39°. This cloud is associated with the California nebula NGC 1499; it extends north-northeast and then, in a very elongated structure, southeast into Auriga, with another strong peak near NGC 1579, a nebula surrounding LkHα 101. Near 4$^{\rm h}$45$^{\rm m}$, 35°, the negative velocity cloud overlaps the Auriga dark clouds (L1492) at 4–5 km s^{-1}, which are smoothly connected to the main Taurus clouds in the center of our map, $\alpha = 4^{\rm h}$–5$^{\rm h}$, $\delta = 20$°–32°.

Two emission ridges, clearer in T_R than in W_{CO}, correspond to the two prominent, filamentary dark nebulae in photographs of Taurus. A moderately strong peak in the northern ridge is in Heiles Cloud 2, which contains TMC-1 and IC 2087; the easternmost peak in the southern ridge is close to TMC-2 in Kutner's cloud (B18). The northern ridge extends from Heiles Cloud 2 through L1495 (B7) northwest to 3$^{\rm h}$40$^{\rm m}$, 31°, where it appears connected to the IC 348 cloud. A chain of clouds with velocities mostly between 5 and 7 km s^{-1} forms an arc east and southeast of the central Taurus region. The last cloud in the chain, L1558, which we only partially mapped, is well separated in velocity at 8–10 km s^{-1} and extends south into the region of the Orion-Monoceros survey (Maddalena *et al.* 1986); the open cluster NGC 1647 lies in this direction. The bipolar outflow cloud L1551 (Knapp *et al.* 1976; Snell, Loren, and Plambeck 1980) at 7 km s^{-1} lies south of the Taurus filaments and in the W_{CO} map appears connected to them by a rather large cloud with higher velocity, $\sim$ 10 km s^{-1}. Southwest of the Taurus and IC 348 clouds is a group of small clouds, partly in Aries, with largely differing velocities; one of these, at 3$^{\rm h}$42$^{\rm m}$, 23°30′, is interacting with the Pleiades (Federman and Willson 1984).

In most of the molecular clouds covered by our survey the equivalent width of the CO line is only 2–3 km s^{-1} (see the false-color map in the lower part of Fig. 3), but it is significantly larger, 5–8 km s^{-1}, in regions of double and multiple lines and star formation, e.g., near IC 348 and NGC 1333. Two major areas found with double or multiple lines are, first, in Auriga, where the Taurus-Auriga clouds at positive velocity overlap the NGC 1499 cloud at negative velocity; and, second, the L1449 region near NGC 1499, which includes many rather small cloud components between −8 and +3 km s^{-1}, some well resolved, others partially blended. To summarize the velocity structure, in Figure 5 we plot the 0.5 K km s^{-1} contour of W_{CO} for all cloud components well separated in space or velocity, with shading to indicate regions of multiple lines or rapid spatial variation of average velocity.

Along the two lines defined in Figure 6a, the detailed velocity structure is shown explicitly in the space-velocity diagrams of Figures 6b and 6c. The line $A'-A''-A'''$ follows the ridge of the long NGC 1499 cloud at negative velocities, passes near NGC 1579, and, at right ascension 4$^{\rm h}$36$^{\rm m}$–5$^{\rm h}$04$^{\rm m}$, cuts through the Auriga clouds at velocities near +5 km s^{-1}; the two velocity components are clearly separated by a deep minimum. The second line, $B'-B''-B'''$, passes through the maxima near NGC 1333 and IC 348 and then follows the northern ridge of the Taurus clouds. It is evident from Figure 6c that (1) the Taurus and IC 348 clouds are connected in velocity, (2) the line widths as well as the overall velocity variation in the IC 348 cloud are much larger than in the Taurus clouds, and (3) a small region near $\alpha = 4^{\rm h}20^{\rm m}$, with velocity $\sim$ 2 km s^{-1}, is overlapped by the Taurus clouds.

For quick reference to individual clouds, we assigned numbers to all extended structures (clouds) and to the most prominent W_{CO} or T_R maxima (peaks). Several peaks found within one cloud are designated by the number of the cloud and a letter, as in Table 1 and Figure 4. The positional accuracy for the peaks is of the order of our beam size, 0°.5, and the definition of some clouds is fairly arbitrary. Clouds only partially mapped, because they are covered by the Columbia second quadrant and Orion surveys, are defined in Figures 4 and 5 by thin broken lines.

IV. DISCUSSION

The mass of a molecular cloud can be estimated from CO observations in two distinct ways, using either an empirical ratio of the CO line intensity to the H_2 column density (CO mass) or the assumption of virial equilibrium between the gravitational potential and the total internal thermal and kinetic energy (virial mass). Both methods require knowledge of the cloud distance r, because the CO mass scales with r^2 and the virial mass with r. Distances also are required to understand the three-dimensional spatial structure of the complexes and to decide whether overlapping objects which appear smoothly connected in W_{CO} and velocity actually are related.

a) Distances

Three methods are commonly used to determine the distances to nearby molecular clouds, all indirect and none highly accurate. The first and generally the best is based on photometric distances to stars thought to be associated with the cloud because they excite an embedded H II region or reflection nebula. The second method is photometry of field
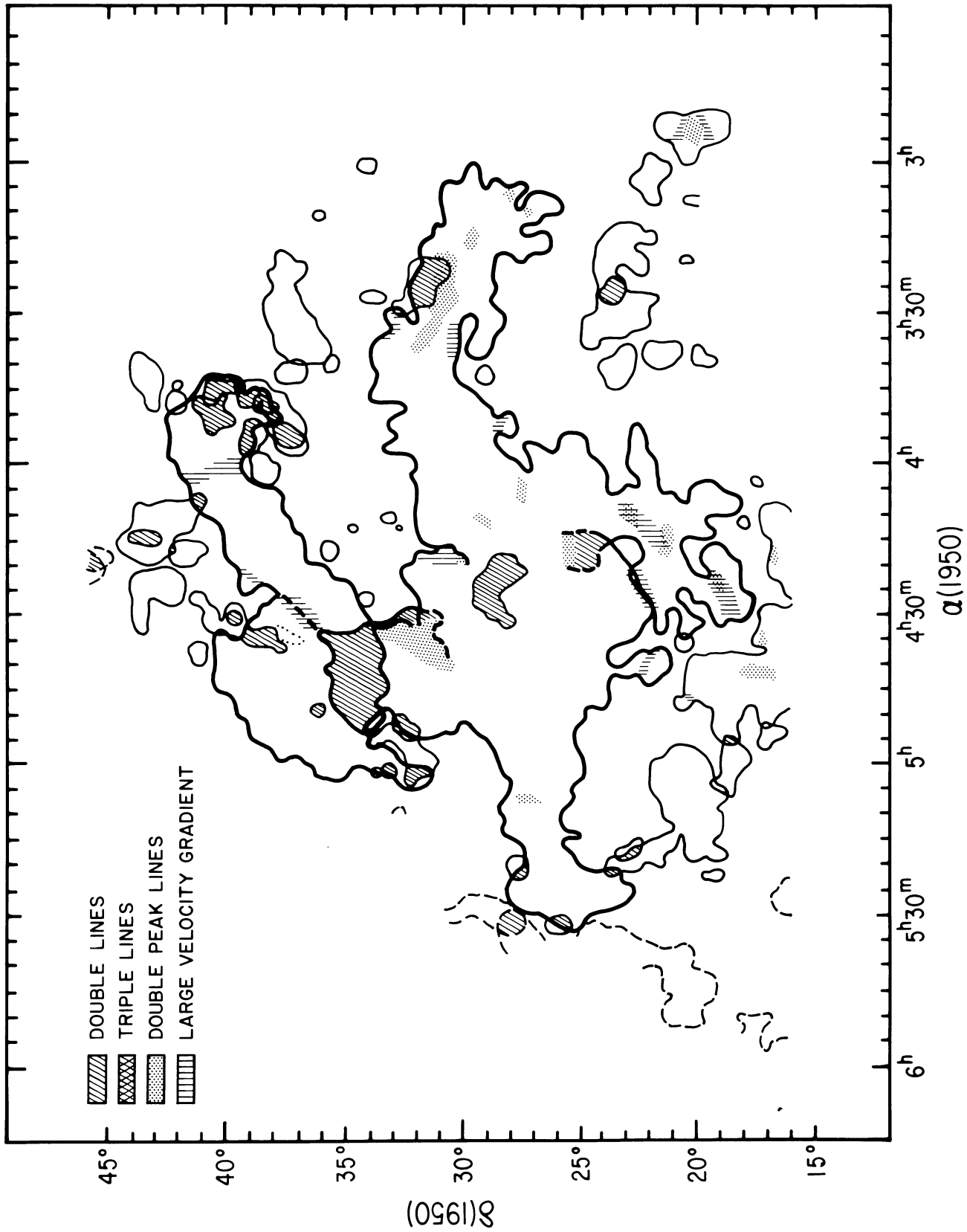
FIG. 5.—Schematic representation of cloud components separated in space or velocity. Cloud outlines correspond to the 0.5 K km s^{-1} level of W_{CO} and are the same as in Fig. 4. Continuous light and dark lines represent fully mapped clouds discussed in this paper. Light dashed lines delineate clouds close to the Galactic plane and in Orion not fully mapped in this survey. Regions of double or triple lines, double-peaked single lines, and steep velocity gradients are indicated by shading.
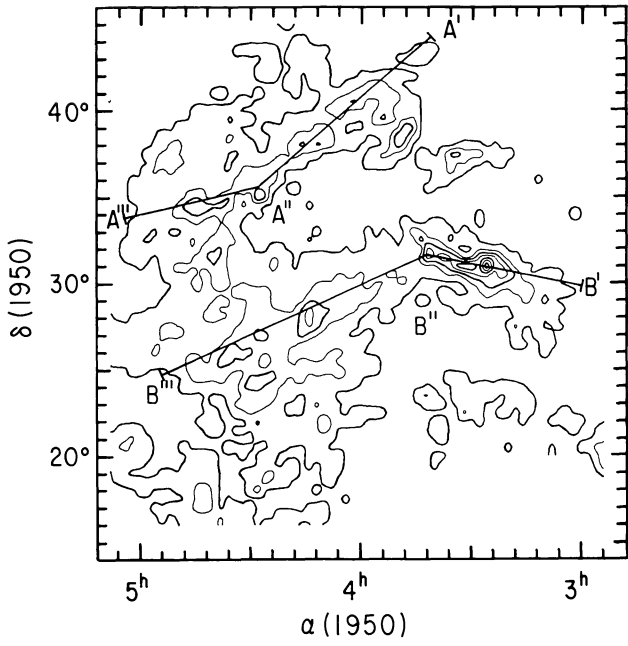
650
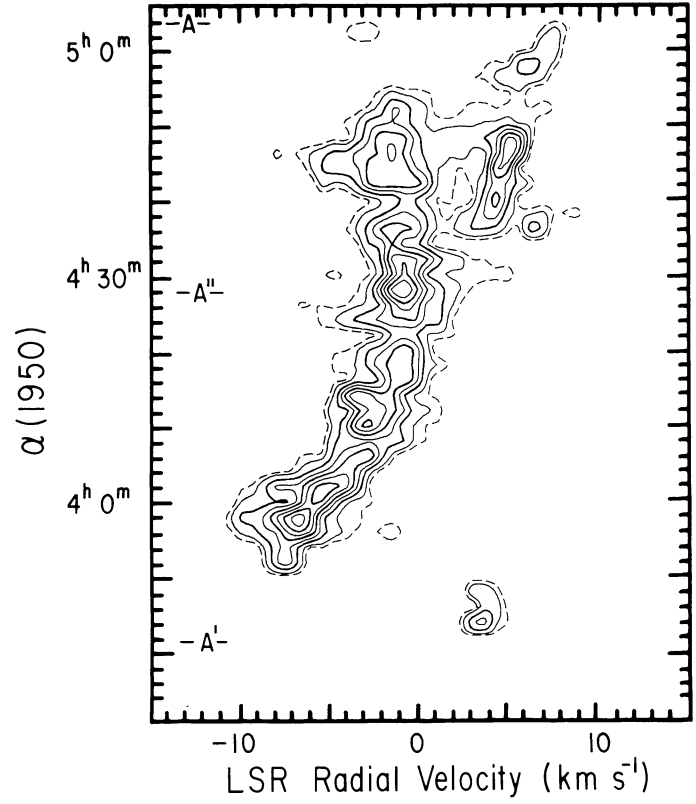
FIG. 6a

FIG. 6b
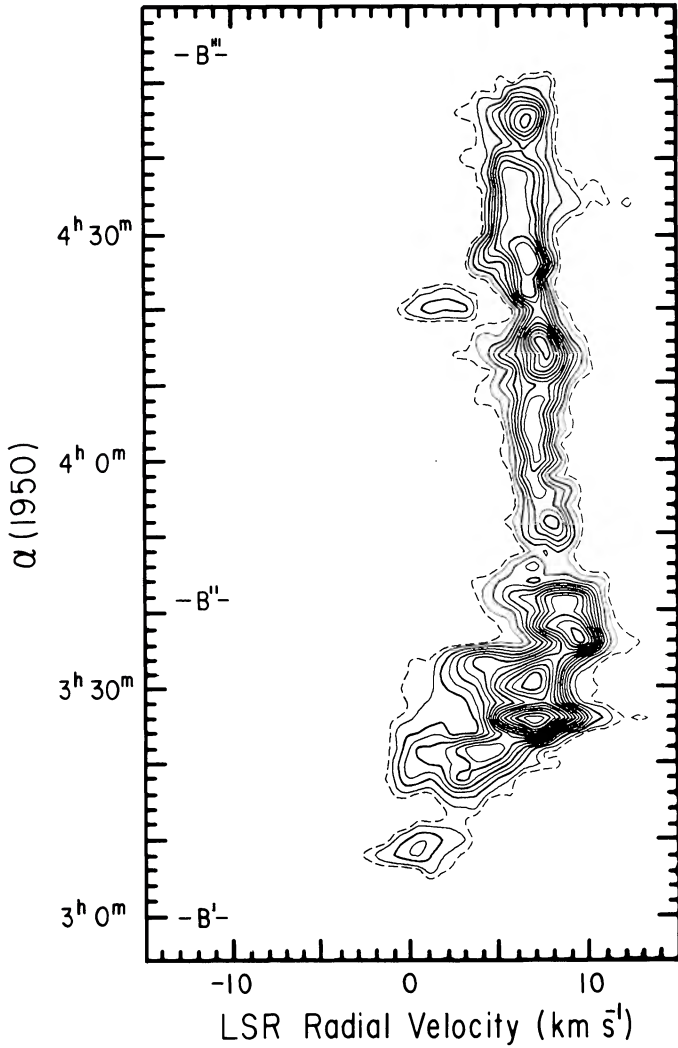
FIG. 6.—Space-velocity diagrams of line temperature T_R along the two cuts shown in Fig. 6a with W_{CO} contours for comparison. (a) The lowest contour for W_{CO} is 0.5 K km s^{-1} (as in Figs. 1, 4, and 5), and the separation between contours is 6 K km s^{-1}. (b, c) The lowest, dashed contour for T_R is 0.25 K, the lowest solid contour is 0.5 K, and the separation between solid contours is 0.5 K.

FIG. 6c

651

TABLE 1
CO EMISSION PEAKS

Peak	α (1950)	δ (1950)	T_R (K)	v_{av} (km s^{-1})	W_{CO} (K km s^{-1})	Related Objects
						Small Clouds in Southwest (Taurus and Aries)
1	2^{h}54^m	20° 00′	2.7	−1.2	12.1	L1453, L1454, L1457, L1458
2	3 02	22 00	1.8	+1.1	4.0	
3	3 26	23 30	1.5	+8.9	3.0	
4	3 32	22 30	2.3	+1.8	7.1	
5	3 38	21 30	2.8	+8.0	4.6	
6	3 38	20 00	0.7	+8.1	1.0	
7	3 42	23 30	3.2	+9.7	6.6	Merope (Pleiades)
						IC 348 Cloud
8a ...	3^{h}26^m	31° 00′	7.8	+6.8	40.1	NGC 1333, L1452, B1, B2, B202–B206, HH 4–HH 12, HH 14–HH 18 IC 348, L1472, B3–B5
8b ...	3 42	32 00	6.2	+8.5	18.4	
8c ...	3 08	28 30	1.2	−0.3	4.1	
8d ...	3 10	26 30	1.0	+1.2	4.2	
8e ...	3 18	27 30	2.2	+2.0	7.1	
8f ...	3 38	29 30	1.2	+8.9	2.0	
9	3 24	31 30	3.2	+2.4	2.0	
						L1434 and L1446
10	3^{h}34^m	37° 30′	2.8	+1.1	13.8	L1434, NGC 1342 (?)
11	3 42	37 00	1.4	+4.2	5.2	L1446
						NGC 1499 Cloud
12a* ..	3^{h}50^m	38° 30′	2.2	−5.0	16.5	L1449, NGC 1499 = S220 (California nebula)
12b ...	3 54	39 30	3.1	−5.9	12.7	[L1443]
12c ...	4 02	40 30	3.2	−5.7	12.8	L1459, L1447
12d ...	4 12	38 00	3.6	−2.7	12.7	L1478, L1473
12e ...	4 28	35 00	4.1	−1.0	18.1	L1478, L1482, LkHα 101, NGC 1579 = S222
12f* ..	4 46	34 30	2.6	−2.1	12.5	L1492
13	4 02	38 00	1.0	+6.3	2.1	
						Small Clouds in North (Perseus)
14	3^{h}46^m	43° 00′	1.8	+3.4	3.7	
15	4 12	42 00	2.3	−1.5	5.3	S214, S215
16* ..	4 16	43 30	1.0	−8.9	1.7	
17	4 18	41 30	1.6	−8.6	3.9	
18	4 24	43 00	1.8	−9.3	4.8	
19* ..	4 32	39 30	1.9	−7.0	3.8	L1479 (?), [L1481]
20	4 38	41 00	0.9	−0.4	2.3	
						Dark Clouds in Auriga
21a ...	4^{h}38^m	38° 00′	2.3	+3.1	6.3	L1481
21b ...	4 54	37 00	3.2	+4.7	9.3	L1488
21c* ..	4 44	35 00	3.5	+4.3	8.3	L1492
22* ...	5 02	33 00	0.9	−9.4	1.8	L1512 (?)
23	5 00	31 30	2.0	−3.9	4.0	L1522 = B222 (?), L1523 = B29 (?)
24a ...	4 42	31 30	3.7	+5.7	12.4	L1505, L1496 = B221, [B26, B27, B28 = L1517, L1519]
24b ...	4 38	30 00	2.6	+4.3	11.9	L1503 = B23, L1507 = B24

TABLE 1 — *Continued*

Peak	α (1950)	δ (1950)	T_R (K)	v_{av} (km s^{-1})	W_{CO} (K km s^{-1})	Related Objects
				Dark Clouds in Taurus		
25	4^h24^m	$31°\,00'$	2.6	+3.8	7.9	
26* ..	4 22	28 00	1.3	+2.0	4.6	L1497 (?)
27a ...	4 32	29 30	3.8	+4.6	10.7	L1500 = B219
27b ...	4 28	27 00	5.0	+5.9	14.2	L1521 = B19
27c ...	4 14	28 00	6.4	+6.9	20.6	L1495 = B7, L1484, IC 359, B209, B211, HH 31
27d ...	4 08	25 30	3.9	+8.1	8.1	L1501, L1498, L1499, L1506, B207, B208, B210, [B212, B215]
27e ...	4 28	24 00	5.8	+6.0	15.3	L1529 = B18, L1542, L1531, L1535, TMC-2, [B212, B215], L1536
27f ...	4 36	25 30	4.8	+6.1	14.6	L1528, L1534, B14, B22, B220, TMC-1, IC 2087
27g ...	4 44	25 00	4.6	+5.9	11.6	L1538
27h ...	4 52	27 30	3.5	+6.0	8.5	L1537, L1539, L1540, L1542, L1544
27i ...	5 14	26 30	3.5	+7.6	7.1	L1545, L1547–L1549, L1552, L1554
27j ...	5 26	23 30	4.0	+7.0	6.2	L1559
28	4 10	22 00	4.0	+10.7	12.0	
29	4 28	18 00	3.9	+7.0	8.6	L1551, S239, L1543, L1546, HH 28–HH 30, [S238, T Tau]
30	4 36	20 30	0.7	+4.2	3.0	
31	4 40	21 30	1.2	+8.5	4.3	L1541 (?)
32	5 04	20 30	4.0	+6.1	7.1	
33	5 00	18 30	1.0	+3.5	2.7	
				L1558		
34	4^h42^m	$17°\,30'$	2.7	+7.9	11.8	L1558, NGC 1647 (?)

NOTE.—Spectra toward the peaks marked with an asterisk show additional lines as follows:

Peak	T_R (K)	v_{av} (km s^{-1})	W_{CO} (K km s^{-1})
12a ...	0.6	+3.1	1.3
12f ...	2.9	+5.0	4.5
16	2.4	−1.3	3.8
19	0.8	+0.6	1.6
21c ...	1.0	−2.7	3.5
22	0.5	+7.4	0.5
26	2.5	+6.8	4.3

stars with spectral or photometric luminosity classification, used to determine the visual extinction A_V or color excess E_{B-V} as a function of the distance to the stars; generally, the opacity of a molecular cloud will cause a steplike discontinuity in E_{B-V} at the distance of the cloud. In the third method, the distance as well as the extinction of a dark cloud are estimated by comparing the number of stars in each magnitude interval toward the cloud and those in an unobscured, nearby standard field. An approximate upper limit to the distance can also be derived for clouds far from the Galactic

plane, because few clouds are expected to be farther from the plane than 3 σ_z, where $\sigma_z \sim 65$ pc is the z dispersion in the Galactic distribution of molecular gas (Dame and Thaddeus 1985). Thus, clouds 10° from the plane are expected to lie within roughly 1 kpc, those 20° from the plane within 600 pc, and those 30° from the plane within 400 pc of the Sun.

Good optical data are available for six star clusters or associations within the region surveyed: the very extended Perseus OB2 association located toward the IC 348 cloud, the CO-free region north of IC 348, and NGC 1499; the young

cluster at IC 348; the open clusters NGC 1342 and NGC 1647; the Pleiades near cloud 7; and the Hyades cluster, widely extended over the southeastern clouds in our survey. The Hyades are so close, $r = 40$ pc (Becker and Fenkart 1971), that they are probably foreground stars unrelated to the molecular clouds in their general direction.

Most authors adopt for IC 348, NGC 1333, and NGC 1499 the distance of the Perseus OB2 association. The star exciting NGC 1499, ξ Per, as well as o Per and BD $+31°643$ near IC 348, were considered by Blaauw (1952) as possible members of Per OB2. Photometric observations of Per OB2 imply distances of 400 pc (Seyfert, Hardie, and Grenchik 1960; Becker and Fenkart 1971), 322 pc (Borgman and Blaauw 1964; Lesh 1969), and 413 pc (Guetter 1977). From photometry of four early-type stars in the IC 348 cluster, Harris, Morgan, and Roman (1954) derived a distance of 380 pc; other estimates are 316 pc from photometry (Strom, Strom, and Carrasco 1974) and 480 pc from proper-motion studies (Frederick 1956). The mean distance to four stars exciting reflection nebulosities in the northern part of the cloud is 330 pc (Racine 1968). Schreur (1970) concluded from star counts that all extinction near NGC 1333 occurs within 500 pc of the Sun, and he obtained the best fit to his data if the obscuring layer is nearer than 300 pc. We adopt 350 pc as the mean distance of the IC 348 cloud and that of the NGC 1499 cloud (L1449).

For the dark Taurus filaments molecular observers, following Elias (1978), generally adopt a distance of 140 pc. This value, first estimated from star counts by Greenstein (1937) and McCuskey (1938, 1939), is consistent with the E_{B-V} versus r relation for stars in a very large field including the Taurus clouds (Gottlieb and Upson 1969), as well as with distances to exciting stars of small nebulosities (Racine 1968). An A_V versus r diagram for 74 stars in the field $\alpha = 4^h20^m - 4^h48^m$, $\delta = 24°.5-27°$ also implies a distance of 140 pc (Straižys and Meištas 1980).

In the region of L1492 and L1488 in Auriga, Eklöf (1958), using photometry of field stars, found two absorbing layers, one at 115 pc, the other at 300–380 pc. It seems reasonable to follow Wouterloot and Habing (1985) in identifying the 115 pc layer with the molecular cloud at positive velocities connected to the Taurus filaments. We adopt 140 pc as the distance of the dark nebulae in Taurus and Auriga, i.e., clouds 21–33. For the calculation of masses we arbitrarily assume that the border between the Taurus clouds and the IC 348 cloud follows the minimal line across the connecting bridge through the saddle point near 3^h45^m, $31°$.

The second absorbing layer found by Eklöf (1958) in Auriga at 300–380 pc is plausibly identified with the eastern end of the NGC 1499 cloud at negative velocities (peak 12f). Heeschen (1951) concluded from star counts that most absorption in the region of our cloud 12 occurs in a layer at 200–300 pc. Ungerer *et al.* (1985) derived the A_V versus r relation for stars in a $2° \times 2°$ field around 3C 111 near peak 12d, and they find that the molecular cloud is at 380 pc. We adopt 350 pc for clouds 12–20, but this distance, too, is uncertain: on the basis of photometry of two B stars, Herbig (1971) estimated that the distance of LkHα 101 (NGC 1579, peak 12e) may be as large as 800 pc. The CO velocity

distribution indicates that the two layers may be spatially connected in some directions: in the space-velocity diagram cutting through the double-line region (Fig. 6b) the two components are connected by weak (0.25–0.5 K) CO emission; in the v_{av} false-color map (Fig. 3, *top*), a smooth velocity transition between the Auriga and the NGC 1499 clouds is seen near 4^h30^m, $38°$, where W_{CO} is less than 2 K km s^{-1}. If these connections are real and not merely a superposition of line wings, the difference in the distances to the two layers is probably small.

The only object toward cloud 10 whose distance has been determined is the open cluster NGC 1342 at 550 pc, with a visual extinction of 0.84 mag (Johnson *et al.* 1961; Becker and Fenkart 1971), whose age according to Gray (1965) is 5×10^8 yr. This great age—and the absence of any apparent interaction between cluster and cloud—suggests that the two are unrelated. On the basis of our present data ($W_{CO} = 2-10$ K km s^{-1}), the extinction caused by the molecular cloud cannot be estimated with sufficient accuracy to say whether NGC 1342 is in front of or behind the cloud. We use a distance of 350 pc, with the reservation that any value between 350 pc (if cloud 10 is indirectly related to Per OB2 and cloud 12) and 800 pc (on the assumption that the distance from the Galactic plane is at most 200 pc) is possible.

The most accurate distance for any object clearly associated with a cloud in our survey is that for the Pleiades, $r = 125$ pc, toward which the extinction is variable but low: $A_V \sim 0.2$ mag (Becker and Fenkart 1971; Crawford and Perry 1976). Cloud 7 is interacting with the Pleiades (Federman and Willson 1984), so we adopted 125 pc as its distance. Apparently, no information is available pertaining to clouds 1–6, but the rather high Galactic latitude ($-25°$ to $-35°$) suggests that they are nearby. We use 125 pc for all these clouds, the scatter in distances probably being high.

The relation of the open cluster NGC 1647 to L1558 (cloud 34) may be analogous to that of NGC 1342 to L1434: the distance is 550 pc, the average absorption 1.2 mag (Becker and Fenkart 1971), and the age 1.3×10^8 yr (Gray 1965). In our survey W_{CO} is close to 6 K km s^{-1}, consistent with the cluster's being behind the cloud, and we adopt a fairly uncertain $r = 500$ pc for cloud 34.

In summary, we use $r = 140$ pc for the Taurus-Auriga clouds on the basis of star counts, distances of reflection nebulae, and E_{B-V} versus r diagrams for field stars; $r = 350$ pc for the IC 348 cloud on the basis of photometry of Per OB2 and IC 348 stars; $r = 350$ pc for the NGC 1499 cloud on the basis of the Per OB2 distance for NGC 1499, the A_V versus r relation toward 3C 111, and studies of the large-scale visual extinction; and, finally, $r = 125$ pc for cloud 7 on the basis of the distance to the Pleiades. The distances to other clouds are poorly known and for the sake of calculation have simply been assumed.

b) Are the Taurus and IC 348 Clouds Connected?

An apparent bridge connecting the northern Taurus filament (L1495) to the IC 348 cloud has long been known from maps of visual extinction (McCuskey 1938, 1939), as well as from undersampled or incomplete molecular-line maps (CO:

Baran 1985; OH: Wouterloot and Habing 1985). The main reason for concluding that these clouds are separate has been the large difference between the distance derived for the Taurus clouds and that for IC 348. Our survey, the first fully sampled, unbiased CO map of this region, confirms the tentative conclusion of Baran (1985) that there is little change in velocity along the bridge. In the false-color map of the average velocity (Fig. 3, *top*) as well as in the space-velocity diagram (Fig. 6c), the Taurus clouds appear smoothly connected to the molecular gas near IC 348.

There is some evidence to suggest that part of the material in the area of B5, IC 348, and the connecting bridge may be significantly closer than 350 pc. The Per OB2 member close to IC 348, o Per, is possibly much nearer than the association, at about 200 pc (Borgman and Blaauw 1964), and the distance derived for IC 348 by Fenkart and Binggeli (1979) from the photometric data of Strom, Strom, and Carrasco (1974) is only 240 pc. Rydgren (1971) concluded from photometry of field stars in the region of B5 and Per OB2 that most absorption in this region occurs within 200 pc of the Sun. Cernicharo, Bachiller, and Duvert (1985) derive 200 pc as an upper limit to the distance of the nearest absorbing layer in the region of IC 348 and NGC 1333 on the basis of the size of the largest dark patches without foreground stars. It is possible, therefore, that a significant amount of molecular gas and extinction lies between 150 and 200 pc, i.e., between the Taurus filaments and the Per OB2 association.

This conclusion, however, fails to answer the question of whether there are two overlapping clouds or one continuous object. If the clouds are connected, the spatial structure and orientation of the bridge must be unusual, unless the adopted distances to IC 348 or NGC 1333, or both, are wrong. We see an apparent change in r from 140 to 350 pc over $<10°$ in projection, corresponding to only 24 and 60 pc at $r = 140$ and 350 pc, respectively. If this change in r is real, the connecting bridge forms an extremely elongated structure along the line of sight, in which case the small variation in velocity, less than 2.5 km s^{-1}, along the bridge is surprising (Fig. 6c). A connecting bridge would be more likely if the difference in distance were not so extreme, e.g., if IC 348 were at $r = 200$–240 pc.

Alternatively, we may consider that a part of the Taurus clouds within 200 pc extends through the region of the bridge into Perseus, causing a significant obscuration in the region of B5 as well as in the largest dark patches between IC 348 and NGC 1333, while the more active molecular clouds associated with IC 348 and NGC 1333—and possibly Per OB2—are separate and farther away (> 300 pc). If so, the IC 348 cloud is not a single object but a chance superposition of several molecular clouds associated with bright nebulae and dark clouds that happen to have nearly equal radial velocities.

c) Masses

With the CO data in hand, it is possible to make the most complete and probably the most accurate estimates to date of the masses of the dark nebulae and associated molecular clouds in Perseus, Taurus, and Auriga. Although the ^{12}CO line is not optically thin, experience shows that, at least if averaged over a typical cloud, the ratio of the intensities of

^{12}CO and ^{13}CO (which is much more nearly optically thin) is fairly constant (Solomon, Sanders, and Scoville 1979; Stark, Penzias, and Beckman 1983). The integral of the CO line intensity over velocity and the two map dimensions, S_{CO}, is therefore approximately proportional to the cloud mass. Calibrating S_{CO} in terms of mass requires observational determination of the average $N(H_2)/W_{CO}$ ratio. The best currently available measurements are based on a correlation analysis of CO, H I, and the *COS B* γ-ray survey over a large part of the sky. Since this analysis has not yet been performed for our survey, we use the ratio $N(H_2)/W_{CO} = 2.6 \times 10^{20}$ cm^{-2} (K km s^{-1})$^{-1}$ derived from Columbia CO survey data for the Orion-Monoceros region by Bloemen *et al.* (1984), a region of local clouds at distances of typically 500 pc. This value is consistent with a similar analysis for large segments of the Galactic plane (Lebrun *et al.* 1983; Bloemen *et al.* 1986), and agrees to within a factor of 2 with results from W_{CO}/A_V ratios (Bloemen *et al.* 1984; Maddalena *et al.* 1986). With a mean atomic weight per H atom of 1.36, we obtain

$$M_{CO}/M_{\odot} = 1.73 \times 10^{-3} r^2 S_{CO}, \tag{1}$$

where r is the distance to the cloud in pc and S is in units of K km s^{-1} deg^2.

For comparison we calculated the virial mass, M_{vir}, assuming virial equilibrium between the gravitational potential and the kinetic energy in the absence of magnetic fields or other sources of pressure. Lacking adequate knowledge of the density structure of the clouds, particularly along the line of sight, we simply used the virial formula for a homogeneous sphere and a Maxwellian velocity distribution:

$$M_{vir} = 5R(\Delta v)^2/(8G \ln 2), \tag{2}$$

where G is the gravitational constant and R the cloud radius, which becomes

$$M_{vir}/M_{\odot} = 209.6r(\Delta v)^2 \tan(A/\pi)^{1/2}, \tag{3}$$

where r is the distance in pc and A the cloud area in square degrees; $\Delta v = 0.94\Delta v_{eq}$ (in units of km s^{-1}) is the FWHM of the CO line obtained by averaging all observed spectra within the cloud.

For selected clouds, Table 2 lists the masses so derived, the mean velocity $\langle v \rangle$ and FWHM Δv of the average spectrum, the angular area, the integrated CO intensity S_{CO}, and the adopted distance, according to the definition of clouds in Table 1 and Figure 4. For clouds not well separated, we use integration boundaries that follow the minimal lines through the valleys and saddle points between the peaks.

Distant objects, in particular the IC 348 and NGC 1499 clouds, account for the largest contributions to the CO mass in our survey, while the near dark clouds in Taurus and Auriga cover the largest area and provide most of the CO flux. The total molecular cloud mass in the survey amounts to almost 2×10^5 $M_{\odot}$. The IC 348 and NGC 1499 clouds have each a mass of about 5×10^4 $M_{\odot}$, or about 50% of the mass of the largest objects in Orion and Monoceros (Maddalena *et al.* 1986). Other estimates of these masses exist: for the IC 348

UNGERECHTS AND THADDEUS

Vol. 63

TABLE 2
CLOUD MASSES

Cloud	$\langle v \rangle$ (km s^{-1})	Δv (km s^{-1})	Area (deg^2)	S_{CO} (K km s^{-1} deg^2)	Distance (pc)	M_{CO} ($10^4 \, M_\odot$)	M_{vir} ($10^4 \, M_\odot$)
1	-1.6	7.4	4.7	19.3	(125)	0.05	[3.1]
2–6 (total)			15.2	30.0	(125)	0.08	...
7	$+9.4$	2.1	1.8	5.1	125	0.01	0.16
8	$+5.3$	8.3	35.8	235	350	4.96	30.1
9	$+1.3$	3.4	2.6	12.9	350	0.27	1.3
10	$+1.0$	4.3	6.4	27.6	(350)	0.58	3.4
11	$+4.6$	3.3	0.8	2.2	(350)	0.05	0.7
12	-3.3	6.4	41.8	263	350	5.55	19.2
14–20 (total)			14.1	31.2	(350)	0.66	...
21	$+4.2$	4.5	34.6	119	140	0.40	3.4
23	-4.2	2.6	2.5	5.0	(140)	0.02	0.31
24	$+5.5$	3.1	20.9	110	140	0.34	1.3
25	$+3.7$	4.4	3.0	11.3	140	0.04	[0.98]
26	$+1.4$	2.4	3.1	8.4	140	0.03	0.29
27	$+6.5$	3.2	128	668	140	2.26	3.25
28	$+10.0$	4.3	18.6	51.5	(140)	0.17	[2.3]
29	$+8.4$	4.1	5.9	18.6	140	0.06	[1.2]
32	$+5.7$	2.4	13.3	38.3	(140)	0.13	0.59
33	$+4.3$	2.7	1.9	3.1	(140)	0.01	0.30
34	$+8.6$	4.0	20.5	68.3	(500)	2.98	7.5
Total	...	...	374	1736	...	18.7	...

NOTE.—Distances in parentheses are uncertain. Virial masses are shown in brackets for clouds with large velocity fluctuations (clumping). Cloud 34 was only partially ($\sim 50\%$) mapped.

cloud, Sancisi et al. (1974), assuming $r = 300$ pc, derive $1.6 \times 10^4 \, M_\odot$ from optical extinction, and Sargent (1979), assuming $r = 330$ pc, obtains $1.2 \times 10^4 \, M_\odot$ from CO. These estimates are based on data limited to the region close to and between NGC 1333 and IC 348 and take into account only about 50% of the area where we detect CO. For the NGC 1499 cloud, Wouterloot and Habing (1985), assuming $r = 300$ pc, derive a mass of $4 \times 10^4 \, M_\odot$ from an OH survey. Given the different sampling and coverage of the maps, these values agree reasonably well; the uncertainty in the distance probably contributes the largest uncertainty in the mass.

The large dark nebulae in Taurus and Auriga at 140 pc (clouds 21 and 24–33), are in angular size the most extensive molecular clouds in the sky; because they are so close, however, their total CO mass is modest, only about $3.5 \times 10^4 \, M_\odot$. The only extensive independent molecular-line map of the Taurus-Auriga clouds is the OH survey by Wouterloot and Habing (1985), who, for a distance of 110 pc, estimate a mass of $1.5 \times 10^4 \, M_\odot$. Since their map does not completely cover our cloud 27, the agreement is as good as could be expected. A rough estimate of the cloud mass is possible also from the low-resolution A_V map of McCuskey (1938, 1939), which shows an average extinction of $A_V = 1.0$–1.2 mag in clouds 24 and 27 and a general distribution similar to our CO map. Assuming that $N(\mathrm{H}_2)/A_V = 0.94 \times 10^{21}$ cm^{-2} mag^{-1} (Bohlin, Savage, and Drake 1978) and that the area of clouds 24 and 27 is 150 square degrees, we obtain $(1.8$–$2.2) \times 10^4 \, M_\odot$, as compared with $2.6 \times 10^4 \, M_\odot$ from CO.

An important result of our survey is the difference between CO and virial masses for most of the clouds. Only in cloud 27, the Taurus cloud, do M_{CO} and M_{vir} agree to 50%.

Elsewhere, e.g., in clouds 8, 10, and 12, M_{vir} is higher than M_{CO} typically by a factor of 4–6; the average of the ratio $M_{\mathrm{vir}}/M_{\mathrm{CO}}$ for the substructures of the Taurus cloud (27a–27j) also is approximately 4, consistent with values derived by Murphy and Myers (1985) from 8$'$ observations of part of cloud 27 (B18 and Heiles Cloud 2). The discrepancy between M_{vir} and M_{CO} would be resolved if the distances were greater by a factor of 4–6 than assumed, but the clouds would then have to be unrealistically far from the Galactic plane, e.g., more than 300 pc in the case of NGC 1499. Alternatively, a higher $N(\mathrm{H}_2)/W_{\mathrm{CO}}$ ratio or any cloud structure implying a lower M_{vir} for the same observed velocity dispersion would decrease $M_{\mathrm{vir}}/M_{\mathrm{CO}}$. Since a value of $N(\mathrm{H}_2)/W_{\mathrm{CO}}$ about twice as high as we used is within the generally accepted range (see, e.g., the discussion in Bloemen et al. 1984), and most of the clouds are nonspherical, we cannot rule out the possibility that these objects are bound. In any case, the more distant clouds are dynamically much more active than the dark clouds in Taurus and Auriga, as indicated by rather broad and multiple lines, e.g., near NGC 1333 and NGC 1499, and by systematic variations in velocity along clouds 8 and 12 as well as, although more irregularly, within clouds 10 and 34.

The ratio of M_{vir} to M_{CO} is even larger, typically 10–30, for the smallest individual clouds, which are more nearly spherical; with about 20 such objects in our survey, only a few are listed in Table 2. They are similar to the small nearby clouds seen by IRAS at high Galactic latitudes, for which the observed CO velocity dispersion exceeds the dispersion expected in virial equilibrium by about a factor of 10 (Blitz, Magnani, and Mundy 1984; Keto and Myers 1986; De Vries,

Heithausen, and Thaddeus 1986). The group L1453, L1454, L1457, L1458 (cloud 1) shows an extremely large line width, 7 km s^{-1}, probably caused by the overlapping and blending of several clumps or clouds at different velocities. Some small clouds in the southeast are included by Magnani, Blitz, and Mundy (1985) in the list of high Galactic latitude clouds, but, as expected, we find several similar objects, e.g., clouds 11, 16–20, and 33, much closer to the Galactic plane.

<center>V. SUMMARY</center>

1. Nearly 50% of the total area surveyed (750 square degrees) shows CO emission, mostly from the nearby (140 pc) dark clouds in Taurus and Auriga. Major clouds at larger distances (350 pc) are the IC 348 cloud and the elongated NGC 1499 cloud at negative velocities extending from Auriga along NGC 1579 to the California nebula (NGC 1499). We also detect several small clouds far off the Galactic plane ($b = -25°$ to $b = -35°$).

2. The accuracy of our mass estimates and our understanding of the structure of the clouds along the line of sight are limited by poor or conflicting information about distances to associated H II regions, reflection nebulae, stars, and star clusters, particularly NGC 1333, o Per, IC 348, Per OB2, ξ Per, NGC 1499, LkHα 101, and NGC 1579. The distance to the Taurus-Auriga clouds is fairly well established at 140 pc (conservatively within the range 100–200 pc). The NGC 1499 cloud, at a distance of 350 pc (250–800 pc), overlaps the Auriga dark clouds but is well separated in velocity. The IC 348 cloud, with an adopted distance of 350 pc, appears

smoothly connected to the Taurus clouds, implying (1) that a bridge about 200 pc long connects the Taurus and IC 348 clouds; or (2) that the distance to IC 348 and NGC 1333 needs to be revised downward to about 200 pc; or (3) that in the region near IC 348 two layers of clumpy clouds are well separated (by 100–200 pc) in space but are very close (< 2 km s^{-1}) in velocity.

3. The IC 348 and NGC 1499 clouds contain most of the molecular cloud mass in our survey, each with about 5×10^4 $M_\odot$ (assuming a distance of 350 pc). The much more extended but nearer Taurus-Auriga clouds contain about $3.5 \times 10^4 M_\odot$.

4. The virial mass for the nearby Taurus clouds is about equal to that derived from the CO luminosity, but that for the IC 348 and NGC 1499 clouds is 4–6 times higher than that derived from their CO luminosity, indicating that these objects are more turbulent, owing to associated star formation, or have large-scale velocity gradients.

5. About 20 small, isolated clouds with masses of order 100 $M_\odot$ have the largest ratio of virial to CO mass: 10–30. They are apparently not gravitationally bound and in this respect resemble the small molecular clouds observed by IRAS at high Galactic latitude.

<center>APPENDIX A</center>

<center>DATA REDUCTION</center>

The 115 GHz CO spectrum toward the dark nebulae in Perseus, Taurus, and Auriga is generally simple, at most locations consisting of a single astronomical emission line at an LSR velocity between -15 and $+15$ km s^{-1}; a single telluric emission line from the mesosphere, at rest in the laboratory frame of reference although generally not in the LSR, also appears during frequency switching, but is subtracted out by position switching. Frequency switching over an interval of either 8 or 6 MHz was used in the present survey; the duration of the cycle was maintained close to 1 s and adjusted automatically, so that the integration time at each grid point within the 0°5×0°5 effective beam is a multiple of the basic signal-reference cycle. The reference phase of the frequency-switching cycle yields negative images of both the astronomical and the telluric lines (Fig. 7, top). Third- or fifth-order polynomial baselines were fitted to the channels without astronomical CO lines and were removed (Fig. 7, middle), and the spectra then folded (Fig. 7, bottom) to increase the signal-to-noise ratio. The lines are much narrower than the full spectral range, which is the range used for the baseline fit. From a comparison of results for different baseline orders or linear baselines over a restricted spectral range, we found that the subtraction of a curved baseline causes errors in the intensities of no more than 5%.

<center>APPENDIX B</center>

<center>COMMENTS ON INDIVIDUAL CLOUDS</center>

<center>I. THE IC 348 CLOUD</center>

Molecular cloud 8, located in the vicinity of the Perseus OB2 association, contains at least two regions of star formation, NGC 1333 and IC 348. Our CO intensities are lower than Sargent's (1979) by a factor of the order of 3, a difference which can probably be attributed to the difference in angular resolution. We do not resolve the peculiar velocity structure around NGC 1333, attributed to a collision between clouds by Loren (1976), or the small region of a bipolar high-velocity flow in L1455 (B204), about 1° south of NGC 1333 (Snell and Edwards 1981; Goldsmith et al. 1984).
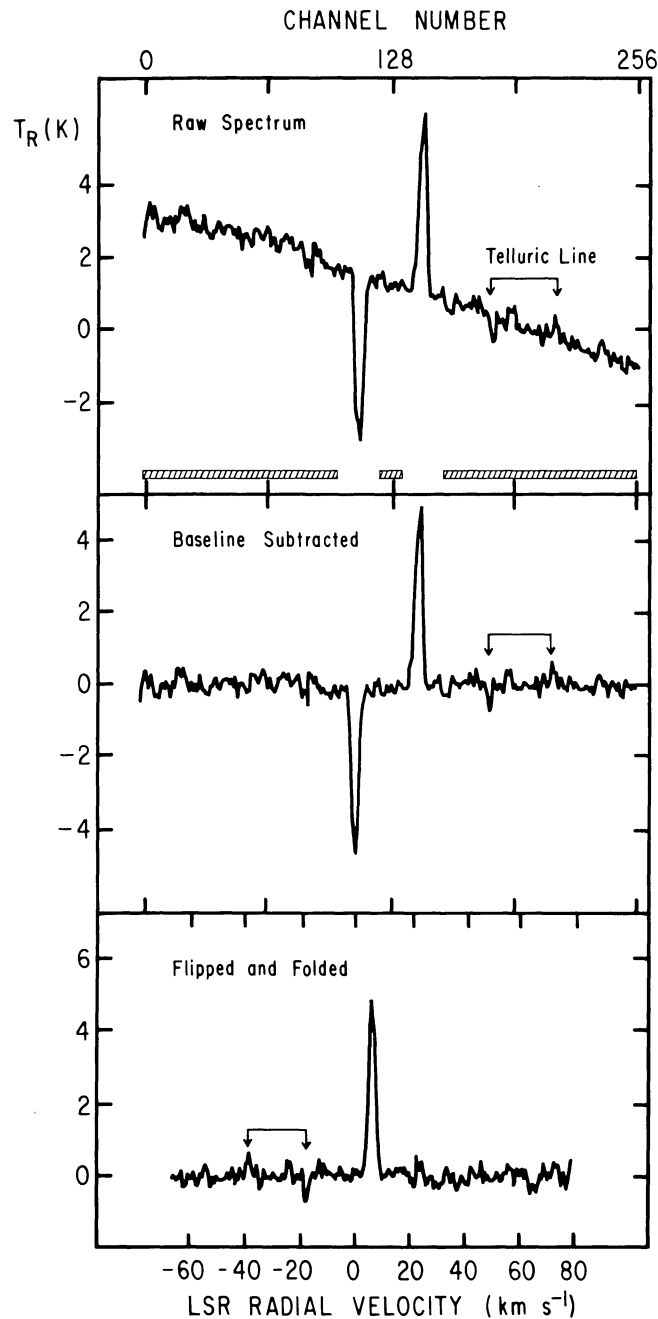
FIG. 7.—A typical spectrum from the survey, obtained at peak 27f near TMC-1: (top) the unprocessed raw spectrum; the crosshatched bars indicate the region fit with a third-order baseline; (middle) the spectrum after baseline subtraction; (bottom) the spectrum flipped and folded to enhance the signal-to-noise ratio.

Several regions in the IC 348 cloud show double peaks, broad lines, or line wings, mainly on the ridge but also in the weak southwest, indicating that the cloud is clumped and turbulent. Only one region, north of NGC 1333, shows line peaks sufficiently separated to suggest the definition of another cloud, cloud 9, which appears as an arc northeast of NGC 1333 in the W_{CO} map (Fig. 1). In our survey the line at the NGC 1333 position is very broad and shows a wing extending down to 0 km s^{-1} (Fig. 6c), including contributions from the possibly colliding clouds and from cloud 9.

II. THE NGC 1499 CLOUD

The California nebula NGC 1499 (or S220), with a length of over 5°, is the only bright, extended H II region in the area of our survey. Its ionization front has apparently reached the dark cloud L1449 to the northwest (Elmegreen and Elmegreen 1978). We find broad lines, single and multiple, at velocities from -8 to $+4$ km s^{-1} in a region that extends from the H II front near 3^h58^m, 37° to 3^h48^m, 41°. Southeast of peak 12c, the velocity increases by 3 km s^{-1} over 2°, and the spectra show close double peaks and asymmetric lines at several positions, suggesting a distinct object with a major peak, 12d, at -2.7 km s^{-1}. Peak 12e is at the position of NGC 1579 (S222), a reflection nebula and compact H II region excited by the luminous emission-line star LkHα 101 (Herbig 1956); the molecular cloud in this region was partially mapped in CO with high angular resolution by Knapp *et al.* (1976). Our survey shows that the NGC 1579 cloud is merely a local maximum in a large cloud complex that extends as far as the California nebula.

III. SMALL CLOUDS TO THE NORTH IN PERSEUS

North of the NGC 1499 complex are several small clouds (14–20), all but one at negative velocities. In the region of cloud 14 the POSS prints show only some diffuse bright nebulosity, LBN 713, LBN 714 (Lynds 1965). In projection on the sky, clouds 15–17 appear connected to each other and to peak 12c (L1459), but they are all well separated in velocity; cloud 18 may be connected to cloud 17 by emission below our detection limit.

IV. DARK CLOUDS IN AURIGA

Several dark clouds north of the Taurus filaments in Auriga are listed by Lynds (1962); some, e.g., L1517 (B26–B28), are compact, with diameters $< 5'$, and quite opaque. This region is filled with molecular clouds 21 and 24, at velocities from 3 to 6 km s^{-1}, somewhat lower than those of the Taurus clouds. The velocities of some compact dark clouds in Auriga are known from observations of NH$_3$ and other molecules that trace high densities, e.g., for L1517 (Benson and Myers 1983; Myers, Linke, and Benson 1983; Gaida, Ungerechts, and Winnewisser 1984). These velocities generally agree well with that of the positive-velocity CO component, suggesting that the dark condensations are embedded in the Auriga CO clouds. Located about 12^m east of peak 24a, B26–B28 (L1517, L1519) are very close to the eastern rim of the molecular cloud, as noted previously from the POSS prints by Schneider and Elmegreen (1979). West and northwest of peak 24a, at $\delta = 30°-33°$, there are blended double lines, which, toward the western border of the cloud, near 4^h34^m, 33°, separate into two clear components at 3 and 7 km s^{-1}.

V. DARK CLOUDS IN TAURUS

The Taurus clouds in the center of our survey contain the filamentary dark clouds with embedded dense cores, such as TMC-1 and TMC-2 (see, e.g., Myers, Ho, and Benson 1979; Benson and Myers 1983; Gaida, Ungerechts, and Winnewisser 1984). The velocity of these cores is known from observations of many molecules, including HC$_5$N and NH$_3$, and most of the CO emission is at the same velocity: $v_{av} = 5-8$ km s^{-1}. We designated the very extended CO cloud in this velocity range as cloud 27; cloud 25, at the northern border of Taurus, and cloud 26 have lower velocities.

The northern optical Taurus filament (B213, B216–B218), very prominent on the photographs but not clearly outstanding in our maps, probably because it is too narrow, is contained in the general CO ridge along B7 (27c), L1521 (27b), and L1528 (27f). The northwestern part of the Taurus clouds is dominated by a broad, strong maximum, 27c, close to L1495 (B7) and IC 359. South of peak 27c a well-defined valley in the CO distribution, where W_{CO} drops below 2 K km s^{-1} before rising again to more than 8 K km s^{-1}, corresponds to the region with low optical extinction between the northern and southern optical filaments. The spectra at some positions in the valley have close double peaks, indicating that the filaments may be separated in velocity by about 1 km s^{-1}.

The southern dark filament includes peak 27d, close to L1501 and B208, and peak 27e, near TMC-2 and B18 (Kutner's cloud). Halfway between peaks 27d and 27e, near B212 and B215, is a peculiar transition between different velocity components: the line at 7–8 km s^{-1} (peak 27d) weakens, and a different line shows up near 4 km s^{-1}; farther east, the 4 km s^{-1} component has a wing or secondary peak at 6 km s^{-1}, and at peak 27e there is only a single, rather narrow line close to 6 km s^{-1}. North of this transition region all components blend into one line at 6 km s^{-1}.

Many molecular-line observations in Taurus have been dedicated to Heiles Cloud 2 around peak 27f near the small bright nebula IC 2087. The embedded dense core TMC-1 is not conspicuous in our survey, owing to the low angular resolution, and one naturally wonders whether other apparently similar peaks in the surrounding molecular clouds are similarly rich in complex molecules. East of Heiles Cloud 2, the dark clouds L1538 (with peak 27g) and L1537, L1539 (with peak 27h) extend over 2° without any visible condensations, while the dark cloud near peak 27i has a good deal of optical fine structure on a 5'–10' scale. Beyond peak 27i, CO emission at velocities near 7 km s^{-1} continues for another 18^m, reaching a last peak, 27j, close to the diffuse, unstructured dark cloud L1559.

Clouds 28–31, south of the central Taurus region, are mostly at somewhat higher velocity, although in W_{CO} they appear connected. Southeast of peak 28 the average velocity remains high, ~ 10 km s^{-1}, so this cloud is well distinguished from the eastern half of the southern filament (peak 27e). About 1°5 west of peak 27j, a narrow bridge of emission appears at $v_{av} = 5$ km s^{-1}, extending southwest to cloud 32, which shows only extremely weak optical extinction. The narrow-line clouds 32 and 33 are rather close in velocity to the central Taurus clouds, so we include them in this category.

REFERENCES

Baran, G. P. 1985, Ph.D. thesis, Columbia University.
Barnard, E. E. 1927, *A Photographic Atlas of Selected Regions of the Milky Way*, ed. E. B. Frost and M. R. Calvert (Washington, DC: Carnegie Institution of Washington).
Baudry, A., Cernicharo, J., Pérault, M., de la Noë, J., and Despois, D. 1981, *Astr. Ap.*, **104**, 101.
Becker, W., and Fenkart, R. 1971, *Astr. Ap. Suppl.*, **4**, 241.
Beichman, C. A., Myers, P. C., Emerson, J. P., Harris, S., Mathieu, R., Benson, P. J., and Jennings, R. E. 1986, *Ap. J.*, **307**, 337.
Benson, P. J., and Myers, P. C. 1983, *Ap. J.*, **270**, 589.
Benson, P. J., Myers, P. C., and Wright, E. L. 1984, *Ap. J.* (*Letters*), **279**, L27.
Blaauw, A. 1952, *Bull. Astr. Inst. Netherlands*, **11**, 405.
Blitz, L., Magnani, L., and Mundy, L. 1984, *Ap. J.* (*Letters*), **282**, L9.
Bloemen, J. B. G. M., Caraveo, P. A., Hermsen, W., Lebrun, F., Maddalena, R. J., Strong, A. W., and Thaddeus, P. 1984, *Astr. Ap.*, **139**, 37.
Bloemen, J. B. G. M., *et al.* 1986, *Astr. Ap.*, **154**, 25.
Bohlin, R. C., Savage, B. D., and Drake, J. F. 1978, *Ap. J.*, **224**, 132.
Borgman, J., and Blaauw, A. 1964, *Bull. Astr. Inst. Netherlands*, **17**, 358.
Bronfman, L., Cohen, R. S., Alvarez, H., May, J., and Thaddeus, P. 1986, *Ap. J.*, submitted.
Broten, N. W., Oka, T., Avery, L. W., MacLeod, J. M., and Kroto, H. W. 1978, *Ap. J.* (*Letters*), **223**, L105.
Cernicharo, J., Bachiller, R., and Duvert, G. 1985, *Astr. Ap.*, **149**, 273.
Cohen, M., and Kuhi, L. V. 1979, *Ap. J. Suppl.*, **41**, 743.
Cohen, R. S. 1978, Ph.D. thesis, Columbia University.
Crawford, D. L., and Perry, C. L. 1976, *A.J.*, **81**, 419.
Dame, T. M., and Thaddeus, P. 1985, *Ap. J.*, **297**, 751.
De Vries, H. W., Heithausen, A., and Thaddeus, P. 1986, *Ap. J.*, submitted.
Dreyer, J. L. E. 1895, *Index Catalogue* (reprinted by the Royal Astronomical Society, 1962).
———. 1888, *New General Catalogue* (reprinted by the Royal Astronomical Society, 1962).
———. 1908, *Second Index Catalogue* (reprinted by the Royal Astronomical Society, 1962).
Duvert, G., Cernicharo, J., and Baudry, A. 1986, *Astr. Ap.*, in press.
Eklöf, O. 1958, *Uppsala Obs. Medd.*, No. 119, in *Ark. Astr.*, **2**, No. 21 (Stockholm: Almqvist & Wiksell), p. 213.
Elias, J. H. 1978, *Ap. J.*, **224**, 857.
Elmegreen, D. M., and Elmegreen, B. G. 1978, *Ap. J.*, **219**, 105.
Federman, S. R., and Willson, R. F. 1984, *Ap. J.*, **283**, 626.
Fenkart, R. P., and Binggeli, B. 1979, *Astr. Ap. Suppl.*, 35, **271**.
Frederick, L. W. 1956, *A.J.*, **61**, 437.
Gaida, M., Ungerechts, H., and Winnewisser, G. 1984, *Astr. Ap.*, **137**, 17.
Goldsmith, P. F., Snell, R. L., Hemeon-Heyer, M., and Langer, W. D. 1984, *Ap. J.*, **286**, 599.
Gottlieb, D. M., and Upson, W. L., II. 1969, *Ap. J.*, **157**, 611.
Gottlieb, E. W., Brock, J. E., and Thaddeus, P. 1986, in preparation.
Gray, D. F. 1965, *A.J.*, **70**, 362.
Greenstein, J. L. 1937, *Ann. Harvard Obs.*, **105**, 359.
Guetter, H. H. 1977, *A.J.*, **82**, 598.
Harris, D. L., Morgan, W. W., and Roman, N. G. 1954, *Ap. J.*, **119**, 622.
Heeschen, D. S. 1951, *Ap. J.*, **114**, 132.
Heiles, C. E. 1968, *Ap. J.*, **151**, 919.
Heiles, C., and Katz, G. 1976, *A.J.*, **81**, 37.
Herbig, G. H. 1956, *Pub. A.S.P.*, **68**, 353.
———. 1971, *Ap. J.*, **169**, 537.
Johnson, H. L., Hoag, A. A., Iriarte, B., Mitchell, R. I., and Hallam, K. L. 1961, *Lowell Obs. Bull.*, **5**, 133.
Jones, B. F., and Herbig, G. H. 1979, *A.J.*, **84**, 1872.
Keto, E. R., and Myers, P. C. 1986, *Ap. J.*, **304**, 466.

Kleiner, S. C., and Dickman, R. L. 1984, *Ap. J.*, **286**, 255.
Knapp, G. R., Kuiper, T. B. H., Knapp, S. L., and Brown, R. L. 1976, *Ap. J.*, **206**, 443.
Kutner, M. L. 1973, in *Molecules in the Galactic Environment*, ed. M. A. Gordon and L. E. Snyder (New York: Wiley), p. 198.
———. 1978, *Ap. Letters*, **19**, 81.
Lebrun, F., *et al.* 1983, *Ap. J.*, **274**, 231.
Lesh, J. R. 1969, *A.J.*, **74**, 891.
Loren, R. B. 1976, *Ap. J.*, **209**, 466.
Lynds, B. T. 1962, *Ap. J. Suppl.*, **7**, 1.
———. 1965, *Ap. J. Suppl.*, **12**, 163.
Maddalena, R. J., Morris, M., Moscowitz, J., and Thaddeus, P. 1986, *Ap. J.*, **303**, 375.
Magnani, L., Blitz, L., and Mundy, L. 1985, *Ap. J.*, **295**, 402.
McCuskey, S. W. 1938, *Ap. J.*, **88**, 209.
———. 1939, *Ap. J.*, **89**, 568.
Murphy, D. C., and Myers, P. C. 1985, *Ap. J.*, **298**, 818.
Myers, P. C. 1982, *Ap. J.*, **257**, 620.
Myers, P. C., Ho, P. T. P., and Benson, P. J. 1979, *Ap. J.* (*Letters*), **233**, L141.
Myers, P. C., Linke, R. A., and Benson, P. J. 1983, *Ap. J.*, **264**, 517.
Palmer, P., Zuckerman, B., Buhl, D., and Snyder, L. E. 1969, *Ap. J.* (*Letters*), **156**, L147.
Pan, S.-K. 1984, Ph.D. thesis, Columbia University.
Penzias, A. A., Solomon, P. M., Jefferts, K. B., and Wilson, R. W. 1972, *Ap. J.* (*Letters*), **174**, L43.
Racine, R. 1968, *A.J.*, **73**, 233.
Rydgren, A. E. 1971, *Pub. A.S.P.*, **83**, 656.
Sancisi, R., Goss, W. M., Anderson, C., Johansson, L. E. B., and Winnberg, A. 1974, *Astr. Ap.*, **35**, 445.
Sargent, A. I. 1979, *Ap. J.*, **233**, 163.
Schneider, S., and Elmegreen, B. G., 1979, *Ap. J. Suppl.*, **41**, 87.
Schreur, J. J. 1970, *A.J.*, **75**, 38.
Seyfert, C. K., Hardie, R. H., and Grenchik, R. T. 1960, *Ap. J.*, **132**, 58.
Sharpless, S. 1959, *Ap. J. Suppl.*, **4**, 257.
Snell, R. L., and Edwards, S. 1981, *Ap. J.*, **251**, 103.
Snell, R. L., Loren, R. B., and Plambeck, R. L. 1980, *Ap. J.* (*Letters*), **239**, L17.
Solomon, P. M., Sanders, D. B., and Scoville, N. Z. 1979, in *IAU Symposium 84, The Large Scale Characteristics of the Galaxy*, ed. W. B. Burton (Dordrecht: Reidel), p. 35.
Stark, A. A., Penzias, A. A., and Beckman, B. 1983, in *Surveys of the Southern Galaxy*, ed. W. B. Burton and F. P. Israel (Dordrecht: Reidel), p. 189.
Straižys, V., and Meištas, E. 1980, *Acta Astr.*, **30**, 541.
Strom, S. E., Strom, K. M., and Carrasco, L. 1974, *Pub. A.S.P.*, **86**, 798.
Sulentic, J. W., and Tifft, W. F. 1973, *The Revised New General Catalogue of Nonstellar Astronomical Objects* (Tucson: University of Arizona Press).
Sume, A., Downes, D., and Wilson, T. L. 1975, *Astr. Ap.*, **39**, 435.
Thaddeus, P., Gottlieb, C. A., Hjalmarson, Å., Johansson, L. E. B., Irvine, W. M., Friberg, P., and Linke, R. A. 1985, *Ap. J.* (*Letters*), **294**, L49.
Thaddeus, P., Vrtilek, J. M., and Gottlieb, C. A. 1985, *Ap. J.* (*Letters*), **299**, L63.
Toelle, F., Ungerechts, H., Walmsley, C. M., Winnewisser, G., and Churchwell, E. 1981, *Astr. Ap.*, **95**, 143.
Ungerer, V., Mauron, N., Brillet, J., and Nguyen-Quang-Rieu. 1985, *Astr. Ap.*, **146**, 123.
Wilson, R. W., Jefferts, K. B., and Penzias, A. A. 1970, *Ap. J.* (*Letters*), **161**, L43.
Wouterloot, J. G. A., and Habing, H. J. 1985, *Astr. Ap. Suppl.*, **60**, 43.

P. THADDEUS: Center for Astrophysics, 60 Garden Street, Cambridge, MA 02138

H. UNGERECHTS: I. Physikalisches Institut der Universität zu Köln, Zülpicher Strasse 77, D-5000 Köln 41, Federal Republic of Germany